

Short communication

Low-temperature heat capacities of $[\text{Er}_2(\text{L-Glu})_2(\text{H}_2\text{O})_6](\text{ClO}_4)_4 \cdot 6\text{H}_2\text{O}(\text{s})$

You-Ying Di ^{a,*}, Jian Zhang ^b, Zhi-Cheng Tan ^{a,b}

^a College of Chemistry and Chemical Engineering, Liaocheng University, Liaocheng 252059, Shandong Province, PR China

^b Thermochemistry Laboratory, Dalian Institute of Chemical Physics, Chinese Academy of Sciences, Dalian 116023, PR China

Available online 6 May 2007

Abstract

A coordination compound of erbium perchlorate with L- α -glutamic acid, $[\text{Er}_2(\text{L-Glu})_2(\text{H}_2\text{O})_6](\text{ClO}_4)_4 \cdot 6\text{H}_2\text{O}(\text{s})$, was synthesized. By chemical analysis, elemental analysis, FTIR, TG/DTG and comparison with relevant literature, its chemical composition and structure were established. The purity was found to be >99.0%, without melting point. Low-temperature heat capacities were measured by a precision automated adiabatic calorimeter from 78 to 318 K. An endothermic peak in the heat-capacity curve was observed over the temperature region of 290–316 K, which was ascribed to a solid-to-solid phase transition. The temperature T_{trans} , the enthalpy $\Delta_{\text{trans}}H_{\text{m}}$ and the entropy $\Delta_{\text{trans}}S_{\text{m}}$ of the phase transition for the compound were determined to be: 308.73 ± 0.45 K, 10.49 ± 0.05 kJ mol⁻¹ and 33.9 ± 0.2 J K⁻¹ mol⁻¹. Polynomial equation of heat capacities as a function of the temperature in the region of 78–290 K was fitted by the least square method.

© 2007 Elsevier B.V. All rights reserved.

Keywords: $[\text{Er}_2(\text{Glu})_2(\text{H}_2\text{O})_6](\text{ClO}_4)_4 \cdot 6\text{H}_2\text{O}$; Adiabatic calorimetry; Low-temperature heat capacity; Phase transition

1. Introduction

A complex of erbium perchlorate with L- α -glutamic acid, $[\text{Er}_2(\text{Glu})_2(\text{H}_2\text{O})_6](\text{ClO}_4)_4 \cdot 6\text{H}_2\text{O}(\text{s})$, was prepared, its structure and composition was determined, low-temperature heat capacity was measured from 78 to 318 K, and thermodynamic parameters about the solid–solid phase transition were calculated. Thermal decomposition of the complex has been studied by TG/DTG.

2. Experimental

2.1. Synthesis and characterization of $[\text{Er}_2(\text{L-Glu})_2(\text{H}_2\text{O})_6](\text{ClO}_4)_4 \cdot 6\text{H}_2\text{O}$

The sample was synthesized by the method given in the literature [1,2].

Er was determined with five duplicate EDTA titrations, and C, N and H by elemental analysis (model, 1160; made in Italy). Values were consistent with those obtained from theoretical calculation, and listed in Table 1. The purity of the sample calculated from the ratio of the Er content to the theoretical content = 99.60%. The composition and structure of the compound

were verified by TG/DTG. FTIR was done to check the coordination of Er with L-glutamic acid and the water in the complex. IR absorption of L- α -glutamic acid and complex (cm⁻¹) are listed in Table 2. FTIR of the complex retained the weak absorption of $-\text{NH}_3^+$, but absorption of $-\text{COOH}$ disappeared, and characteristic vibration absorption of two $-\text{COO}^-$ appeared, indicating that the amino acid is coordinated as a mononegative ion. $\nu_{(\text{COO}^-)}^{\text{as}}$ and $\nu_{(\text{COO}^-)}^{\text{s}}$ in α and γ places were shifted to low wave numbers, respectively. The symmetrical stretching vibration of α -carboxyl in the complex was a single peak, but that of γ -carboxyl was split into double peaks. This showed that two carboxyls of L- α -glutamic acid in the complex took part in the coordination. The complex has the very strong absorption of water $\nu_{\text{O-H}}$, a very wide and scattered absorption peak of $\nu_{\text{O-H}}$ indicated that both the crystal and coordinated waters existed in the complex.

In addition, TG–DTG technique was applied to determine the stability of the compound, as shown in Fig. 1.

2.2. Adiabatic calorimetry

A high-precision automatic adiabatic calorimeter was used to measure the heat capacities over the temperature range 78 K $\leq T \leq$ 318 K. The principle and structure of the adiabatic calorimeter were described in detail elsewhere [3].

* Corresponding author. Fax: +86 635 8239121.

E-mail addresses: yydi@lcu.edu.cn, diyuying@126.com (Y.-Y. Di).

Table 1

The results of chemical and elementary analysis for Er, C, N and H of the sample (weight%)

	Elements			
	Er	C	H	N
Measured	26.85	9.62	3.23	2.24
Calculated	26.96	9.68	3.25	2.26

To verify the accuracy of the calorimeter, the heat-capacity of α -Al₂O₃, were made at $78\text{ K} \leq T \leq 373\text{ K}$. The sample mass used was 1.6382 g. Deviations of the experimental results from those of the smoothed curve were within $\pm 0.2\%$, while the uncertainty was within $\pm 0.3\%$, as compared with the values given by the former National Bureau of Standards [4] over the whole temperature range.

Heat-capacity measurements were continuously and automatically carried out by means of the standard method of intermittently heating the sample and alternately measuring the temperature. The heating rate and temperature increments were generally controlled at $0.1\text{--}0.4\text{ K min}^{-1}$ and $1\text{--}3\text{ K}$. The heating duration was 10 min, and the temperature drift rates of the sample cell measured in an equilibrium period were always kept within 10^{-3} to $10^{-4}\text{ K min}^{-1}$ during the acquisition of all heat-capacity data. The data of heat capacities and corresponding equilibrium temperature have been corrected for heat exchange of the sample cell with its surroundings [3]. The sample mass used for calorimetric measurements was 2.6111 g, which was equivalent to $2.105 \times 10^{-3}\text{ mol}$ in terms of its molar mass, $M = 1240.72\text{ g mol}^{-1}$.

3. Results and discussion

3.1. Heat capacity

All experimental results were listed in Table S1 (see supplementary data) and plotted in Fig. 2. An obvious endothermic peak appeared in the temperature region from 290 to 316 K. No

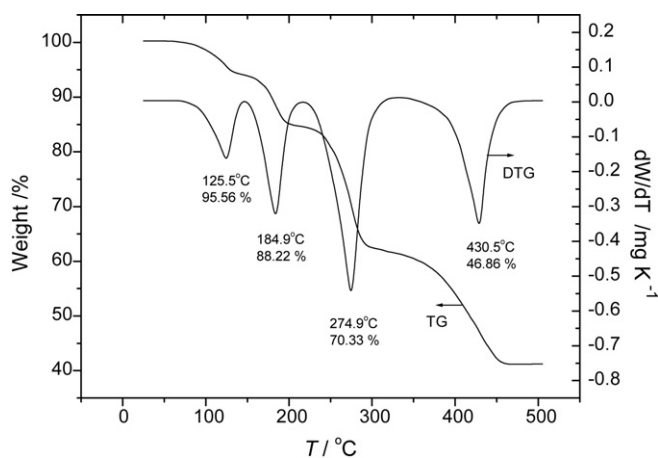


Fig. 1. TG/DTG curve of the complex $[\text{Er}_2(\text{L-Glu})_2(\text{H}_2\text{O})_6](\text{ClO}_4)_4 \cdot 6\text{H}_2\text{O}(\text{s})$.

Table 2
Data of IR absorption of main groups of L- α -glutamic acid and target complex (cm^{-1})

Compound	$\nu_{\text{O-H}}(\text{H}_2\text{O})$	$\nu_{\text{NH}_3^+}^{\text{as}}$	$\nu_{\text{NH}_3^+}^{\text{s}}$	$\nu_{(\text{COO}^-)}^{\text{as}}$	$\nu_{(\text{COO}^-)}^{\text{s}}$	$\nu_{(\text{COO}^-)}^{\text{as}}$	$\nu_{(\text{COO}^-)}^{\text{s}}$	$\nu_{(\text{COO}^-)}^{\text{as}}$	$\nu_{(\text{COO}^-)}^{\text{s}}$	$\nu_{\text{O-H}}(-\text{COOH})$
L- α -Glu	/	3150 (m, s)	2910 (br, m)	1690 (vs)	1640 (m)	1580 (vs)	1540 (s)	1460 (m)	1422 (m)	2650 (m)
Complex	2800–3600 (br, vs)	2720 (vw)	2630 (vw)	1630 (vs)	1530 (s)	1470 (s)	1420 (vs)	1310 (m)	1250–1270 (m)	/

br—broad peak; s—strong; m—middle; w—very weak; vs—very strong; ν —stretching vibration; δ —bending vibration; s—symmetrical; as—asymmetrical.

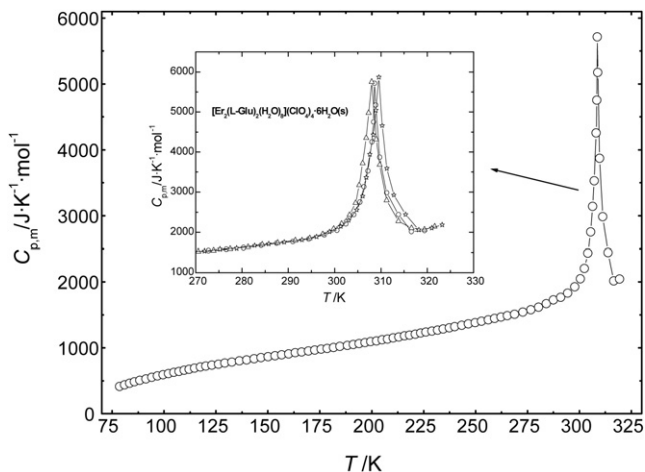


Fig. 2. Experimental molar heat-capacity curve of the complex $[\text{Er}_2(\text{L-Glu})_2(\text{H}_2\text{O})_6](\text{ClO}_4)_4 \cdot 6\text{H}_2\text{O}(\text{s})$ with the temperature (K) in which “○” represents the first series of heat-capacity measurements; “△” represents the second series of heat-capacity measurements; and “☆” represents the third series of heat-capacity measurements.

melting took place in the temperature range, as shown by micro-melting point device. No mass-loss phenomenon occurred in the temperature region by TG/DTG analysis. Therefore, the endothermic peak may be attributed to a solid–solid phase transition of the sample.

The heat capacity of the sample increased with the temperature in the temperature regions of 78–290 and 316–371 K. The heat capacity increased at a higher rate above $T = 318$ K, which is related to the slow dehydration of the coordination compound, which also means the heat capacities are meaningless. Experimental molar heat capacities in 78–290 K were fitted to a polynomial of heat capacities with the reduced temperatures by least square fitting,

$$C_{p,m} = 1016.0 + 509.90x + 147.14x^2 + 18.191x^3 - 252.48x^4 + 140.45x^5 + 170.87x^6$$

in which x was the reduced temperature, and $x = (T - 184)/106$. The relative deviations of the smoothed heat capacities obtained by the above equation from the experimental heat capacities were within $\pm 0.40\%$ except for several points around the lower and upper temperature limits.

3.2. Peak temperature, enthalpy and entropy of the solid–solid phase transition

Three series of heat-capacity experiments in the temperature region of $T = 250$ – 350 K were made to confirm the reversibility and repeatability of the phase transition. Before each series of measurements, the sample was cooled from $T = 350$ to 250 K by using liquid nitrogen as the coolant and introducing helium gas to the vacuum can of the calorimeter.

The area of the peak of the solid–solid transition equaled to heat quantity absorbed by the phase transition of the sample. The molar enthalpy of the transition [5] can be calculated from

Table 3

The results of solid–solid phase transition of the compound obtained from three series of heat-capacity measurements

Thermodynamic properties	x_1	x_2	x_3	$\bar{x} \pm \sigma_a^a$
T_{trans} (K)	308.63	308.01	309.55	308.73 ± 0.45
$\Delta_{\text{trans}}H_m$ (kJ mol^{-1})	10.41	10.60	10.45	10.49 ± 0.05
$\Delta_{\text{trans}}S_m$ ($\text{J K}^{-1} \text{mol}^{-1}$)	33.7	34.4	33.8	33.9 ± 0.2

^a $\sigma_a = \sqrt{\sum_{i=1}^3 (x_i - \bar{x})^2 / n(n-1)}$, in which n is the experimental number; x_i a single value in a set of dissolution measurements; and \bar{x} is the mean value of a set of measurement results.

the following equation:

$$\Delta_{\text{trans}}H_m = \frac{Q - n \int_{T_i}^{T_{\text{trans}}} C_{P(s,I)} dT - n \int_{T_{\text{trans}}}^{T_f} C_{P(s,II)} dT - \int_{T_i}^{T_f} \bar{H}_0 dT}{n} \times (\text{J mol}^{-1}) \quad (1)$$

where T_{trans} is the peak temperature of the transition of the sample; T_i the equilibrium temperature slightly below the beginning transition temperature; T_f the temperature a little higher than the ending transition temperature; Q the total energy introduced to the sample and cell when heating up from T_i to T_f ; \bar{H}_0 the average heat capacity of empty cell between T_i and T_f ; $C_{P(s,I)}$ the heat capacity at T_i ; $C_{P(s,II)}$ the heat capacity at T_f ; and n is the molar number of the sample.

The molar entropy of the transition can be calculated based on molar enthalpy and peak temperature of the transition by the formula:

$$\Delta_{\text{trans}}S_m = \frac{\Delta_{\text{trans}}H_m}{T_{\text{trans}}} \quad (2)$$

The results of T_{trans} , $\Delta_{\text{trans}}H_m$ and $\Delta_{\text{trans}}S_m$ obtained from three series of repeated heat-capacity measurements were shown in Table 3.

Acknowledgement

This work was financially supported by the National Science Foundation of China under the contract NSFC No. 20673050.

Appendix A. Supplementary data

Supplementary data associated with this article can be found, in the online version, at doi:10.1016/j.tca.2007.05.002.

References

- [1] W.-C. Yang, R.-Y. Wang, T.-Z. Jin, Z.-Y. Zhou, X.-G. Zhou, *J. Rare Earths* 16 (2) (1998) 11–17.
- [2] Z.-L. Wang, N.-H. Hu, C.-L. Niu, K.-Y. Yang, J.-Z. Ni, *Chin. Chem. Lett.* 2 (12) (1991) 961–962.
- [3] Z.-C. Tan, G.-Y. Sun, A.-X. Yin, W.-B. Wang, J.-C. Ye, L.-X. Zhou, *J. Therm. Anal.* 45 (1995) 59–67.
- [4] G.A. Donald, *J. Phys. Chem. Ref. Data* 22 (6) (1993) 1441–1449.
- [5] J. Xing, Z.-C. Tan, Y.-Y. Di, X.-H. Sun, L.-X. Sun, T. Zhang, *Acta Chim. Sin.* 62 (24) (2004) 2414–2419 (in Chinese).